



## Detection and dissolution of sparingly soluble SrS and CaS particles in aqueous media depending on their size distribution

Kalev Uiga\*, Ergo Rikmann, Ivar Zekker, and Toomas Tenno

Institute of Chemistry, University of Tartu, Ravila 14a, 50411 Tartu, Estonia

Received 1 July 2020, accepted 3 September 2020, available online 20 October 2020

© 2020 Authors. This is an Open Access article distributed under the terms and conditions of the Creative Commons Attribution-NonCommercial 4.0 International License (<http://creativecommons.org/licenses/by-nc/4.0/>).

**Abstract.** The aim of the current study is to investigate the dissolution process of alkaline-earth metal sulfides SrS and CaS in ultrapure MilliQ water and define the size dependence of the formed particles on the amount of added salt due to the similarity of their chemical properties (e.g. a cubic crystal structure, ion radius). The pH values of SrS and CaS aqueous solutions increased when an additional amount of salt was added into these closed equilibrium systems, as the average quantity and size of the formed particles rose respectively in the measured range of 10–1500 nm. The nanoparticles (detected by Nanosight® LM10) appeared in the prepared aqueous solutions containing  $0.092 \pm 0.01$  mM of SrS<sub>(s)</sub> (pH =  $9.97 \pm 0.02$ ) and  $0.097 \pm 0.01$  mM of CaS<sub>(s)</sub> (pH =  $9.94 \pm 0.02$ ) or above the aforesaid salt amount, which was about 18 times lower concentration than our previously determined values for [SrS] = 1.671 mM and [CaS] = 1.733 mM (pH =  $11.22 \pm 0.04$ ). Up to these amounts of added salt in the closed equilibrium systems of H<sub>2</sub>O–SrS and H<sub>2</sub>O–CaS, all particles had dissolved due to the better solubility of smaller ones, which is related to their larger specific surface area, and thus, to the increase in solubility. Therefore, this principle allows to calculate the value of the solubility product ( $K_{SP}$ ) for nanoscale particles in different equilibrium systems by using the nanoparticle tracking analysis (NTA) method.

**Key words:** strontium sulfide (SrS), calcium sulfide (CaS), solubility product ( $K_{SP}$ ), Nanosight® NTA (nanoparticle tracking analysis).

### 1. INTRODUCTION

Strontium (Sr) and calcium (Ca) are elements collectively known as alkaline-earth metals, which have similar chemical properties (e.g. a cubic crystal structure, ion radius: 99 pm and 113 pm, respectively). Both SrS and CaS have a sodium chloride (NaCl) type of a cubic crystal structure, indicating that the bondage in these salts is highly ionic. They are generally slightly soluble in water, insoluble in alcohol and soluble in acids with decomposition [1]. Minor solubility is caused by strong attractive forces between ions in the crystal structure, from where they could be separated by the energy released from the solvation process [2]. Thus, the dissolution of solid particles in a

liquid is dependent on the dissociation and diffusion of solute molecules towards the liquid phase [3,4].

Strontium compounds, including SrS (strontium sulfide), are formed as by-products in several industrial processes (e.g. metallurgy and energy production), although their practical usage is quite limited (mainly used for fireworks, ceramics, luminous paints and depilatories) [5]. SrS dissociates and forms Sr<sup>2+</sup>, S<sup>2-</sup>, HS<sup>-</sup> (bisulfide H<sub>2</sub>S<sub>(w)</sub>) in deoxygenated aqueous media [6].

Calcium sulfide occurs in nature as mineral oldhamite. It is used in luminous paints and as a precipitation agent for trace metals in the acidic wastewater effluent treatment [7,8]. There are only a few published data about the solubility of CaS because it is stable only in the dry solid form. Apart from technological synthesis, CaS is generated in the retorting process of oil shale containing pyrite

\* Corresponding author, [kalevu@gmail.com](mailto:kalevu@gmail.com)

and other sulfides. In addition, more than 50% of the initial sulfur in Estonian oil shale remains as solid residue, called semi-coke (it contains 1.7–2.1% sulfur), where its interaction with water generates highly alkaline leachate and the formation of toxic  $\text{H}_2\text{S}$  under anaerobic conditions. [9–11]. Although SrS and CaS are only slightly soluble in water, their reaction with it causes a significant pH increase that could pose a high environmental hazard [6,9].

After dissolution of solid SrS or CaS, the formed particles are surrounded by an aqueous medium as their solvation (or hydration when the solvent is water) and dissociation into ions takes place in the liquid phase. Addition of energy by rising the system's temperature is required to overcome intermolecular interactions (e. g. van der Waals and electrostatic forces) that occur in a solute. The unequal charge distribution in polar liquids, such as water, where the interactions between molecules in a liquid are constantly breaking and reforming, makes them good solvents for ionic compounds, including sparingly soluble SrS and CaS. As a result of their hydration process, the partially negatively charged oxygen atoms of the  $\text{H}_2\text{O}$  molecules surround the cations ( $\text{Sr}^{2+}$  or  $\text{Ca}^{2+}$ ) and the partially positively charged hydrogen atoms in  $\text{H}_2\text{O}$  surround the anions ( $\text{S}^{2-}$ ), as seen in Fig. 1 [12,13].

Furthermore, the pH of the SrS or CaS aqueous solution is a key parameter in evaluating interactions between the adsorbate and the adsorbent, as it provides information that allows optimization of the conditions for the adsorption system. The adsorbent and the adsorbate must be oppositely charged to provide a larger electrostatic interaction between them. Lower adsorption in the acidic solutions is attributed to protons competing with metal ions for the exchange of places [12,14,15].

According to Zumdahl [16], the aqueous solubility of sparingly soluble compounds in equilibrium with the solid

phase is constant and it corresponds to the value of  $K_{\text{SP}}$  only when no chemical reaction takes place in the water phase. The product of molar concentrations of the ions formed in the dissolution has an infinite number of possible values, depending on the conditions, such as the presence of a common ion and the temperature [16]. Thus, chemical precipitation or dissolution occurs when the concentration of ions in the aqueous phase exceeds or is less than the solubility, respectively. The supersaturation or undersaturation of a sparingly soluble mineral is an important concept in the prediction of the potential for mineral precipitation or dissolution to occur [17].

Proton-centred models have been developed for the closed self-regulating systems of  $\text{H}_2\text{O}$ –SrS and  $\text{H}_2\text{O}$ –CaS. Previous studies have shown that when solid SrS or CaS is added into deoxygenated water, the pHs of these closed equilibrium systems will increase and the achieved constant value will be dependent on the added amount of salt. Moreover, the final pH values of these equilibrium systems have corresponded to the model-predicted ones [6,9]. However, the abundance of nanoparticles (with the dimensions in the size range between 1 and 100 nm) in the equilibrium systems results in a faster rise of the system's pH values due to their larger specific surface area [18,19].

The Kelvin equation has also been applied to determine the equilibrium solubility of solids in a liquid. The ratio of vapour pressures is dependent on the solubility of the spherical and flat particles, but the surface tension  $\mu$  used for the gas-liquid interface can not be applied for an interface involving solids and it may be written in the following form (Eq. 1) [12,20]:

$$RT \ln \left( \frac{a}{a_0} \right) = (m + n) RT \ln \left( \frac{S}{S_0} \right) = \frac{2MY}{\rho R S} \quad [12], \quad (1)$$

where  $a_0$  is the activity of the dissolved solute in equilibrium with a flat surface, and  $a$  is the analogous quantity for a spherical surface;  $S$  and  $S_0$  are shown as molar solubilities of the spherical and flat particles, respectively;  $\gamma$  denotes chemical potential ( $\text{J}\cdot\text{m}^{-2}$ );  $\rho$  refers to density;  $R$  is the ideal gas constant ( $\sim 8.314 \text{ J}\cdot\text{K}^{-1}\cdot\text{mol}^{-1}$ ).

The surface free energy interpretation of  $\gamma$  is more plausible for solids than the surface tension interpretation, which is useful for liquid interfaces. Although the increase in the solubility of small particles is unquestionably a real effect, using it quantitatively for evaluating the precise value of  $\gamma$  is difficult [12]. The generally accepted concept is that neither the amount of excess solid nor the size of the particles present in the system will change the position of the equilibrium [21].

Theoretical explanations are so far mainly based on thermodynamics, which underestimates the interaction between the particles of the solvent and the soluble matter, as well as the interparticle interactions occurring within

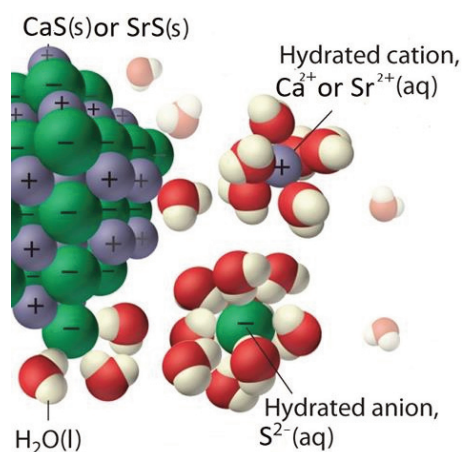


**Fig. 1.** Dissolution and hydration of solid SrS and CaS particles in aqueous media.

the phases of each environment and the interface of the phases. In the case of a smaller diameter of the solid-phase particles, the curvature of their surface is larger, and thus, the particles on the surface are weakly bound to the ones in the inner and side layers of the solid phase and can more easily transfer from the solid to the liquid phase. By dissolution of salts and dissociation of water these processes are affected by ionic radius and many intermolecular forces, including hydrogen bonding, dipole-dipole, and van der Waals forces. Chemical reactions occurring in the liquid phase lead to a new equilibrium to be established in this phase and thereby will also change the existing balance on the boundary surface of the solid-liquid phase [12].

Nanoparticle tracking analysis (NTA) provides direct and real-time visualization, sizing, and counting of particulate materials in the size between 10 and 2000 nm in liquid suspension by using only a metallized optical element illuminated by a laser beam of a conventional optical microscope fitted with an inexpensive camera and a dedicated analytical software package. This technique works on a particle-by-particle basis, relating the degree of movement under Brownian motion to the sphere equivalent hydrodynamic diameter particle size, allowing high resolution particle size distributions and counting to be obtained within minutes. The instrument generally records a video of the moving particles at a given frame rate, which allows for determination of the location of all the particles in the observation area for each recorded frame. This enables the software to construct a dynamic model for the observed particles, including their movement tracks and the number of steps to be taken to cover the distance [22–27]. The computer program analyses each frame of the video, determining the location of the observed particles by applying a modified Stokes–Einstein equation (Eq. 2) to calculate the hydrodynamic diameters of each individual particle as follows:

$$\overline{(x, y)^2} = \frac{2k_B T}{3r_h \pi \eta} \quad [26], \quad (2)$$

where  $k_B$  is the Boltzmann constant and  $\overline{(x, y)^2}$  is the mean squared speed of a particle at a temperature  $T$ , in a medium of viscosity  $\eta$ , with a hydrodynamic radius of  $r_h$ . NTA is widely used as a preliminary characterization technique prior to their exposure and it has been applied to a wide range of materials, including metals, metal oxides, and polymers [22,26,27].

The aim of the current study is to examine the role of nanoparticles in the process of the dissolution of sparingly soluble compounds, such as SrS and CaS by, using NTA as a new characterization method for their analysis. Moreover, previous studies have shown that this technique is very accurate for sizing both monodisperse and polydisperse samples because it has a substantially better

peak resolution compared to other similar methods [19,26].

## 2. MATERIALS AND METHODS

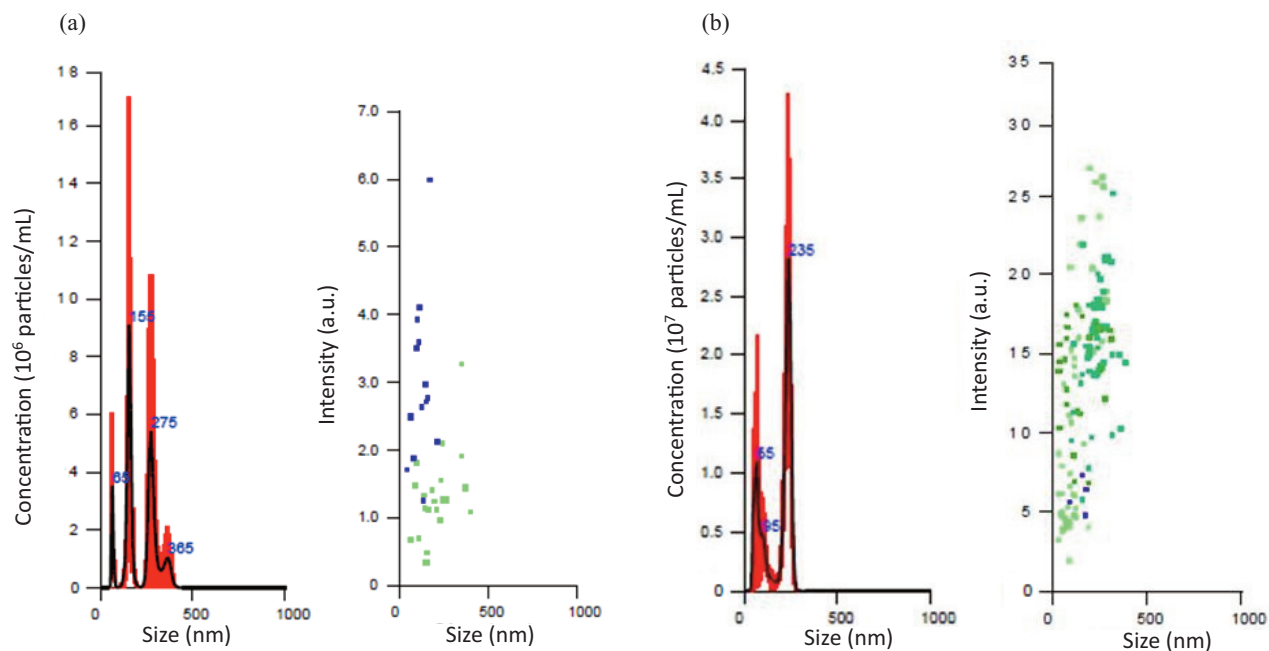
The experiments were carried out at normal pressure (101325 Pa) in air-tightly closed glass bottles (with a volume of 1200 mL), which were filled with purged (for ca 30 minutes with 99.999% Ar) MilliQ ultrapure water and inserted into a thermostated water bath (Assistant 3180, Germany) equipped with a magnetic stirrer (Stuart Scientific magnetic stirrer SM5) in order to keep a constant temperature of  $25 \pm 0.2$  °C and a stirring speed of about 200 rpm during measurements. The efficiency of deoxygenation was controlled by the measurements of dissolved oxygen (DO) in water (oxygen-meter Marvet Junior MJ2000, Elke Sensor, Estonia).

Solid SrS and CaS (99.9%, Alfa Aesar, Germany) were weighed with analytical balance (Scaltec SBC 31, Germany; measuring accuracy of  $\pm 0.001$  g). The pH was measured potentiometrically in at least three replicates by using a pH meter (Jenway 3520, UK), which was connected to a pH electrode (Jenway model No. 924-076, standard error of  $\pm 0.003$ ) intended for highly alkaline solutions. It was calibrated before each measurement at pH values of 7.00, 10.00, and 13.00 in buffer solutions with a standard error of  $\pm 0.002$ . The pH electrode was inserted tightly into the closed reaction cell which was connected with a computer controlled pH measurement program (Dataway version 1.1; JENWAY, UK) registering the corresponding pH values of SrS and CaS aqueous solutions.

In order to count and measure the particle sizes in aqueous media, their detection and tracking analysis was carried out by applying standard measurements of the NanoSight LM10 viewing unit (Malvern Instruments Ltd., United Kingdom). The measurements were made at a controlled temperature of 25 °C by using a cuvette, where the prepared samples of known concentrations of SrS and CaS aqueous solutions were carefully injected in order to avoid the formation of nanobubbles, which may affect the obtained results. For each measurement, the prepared samples were injected five times with three repetitions in order to obtain results with a sufficient confidence level [26].

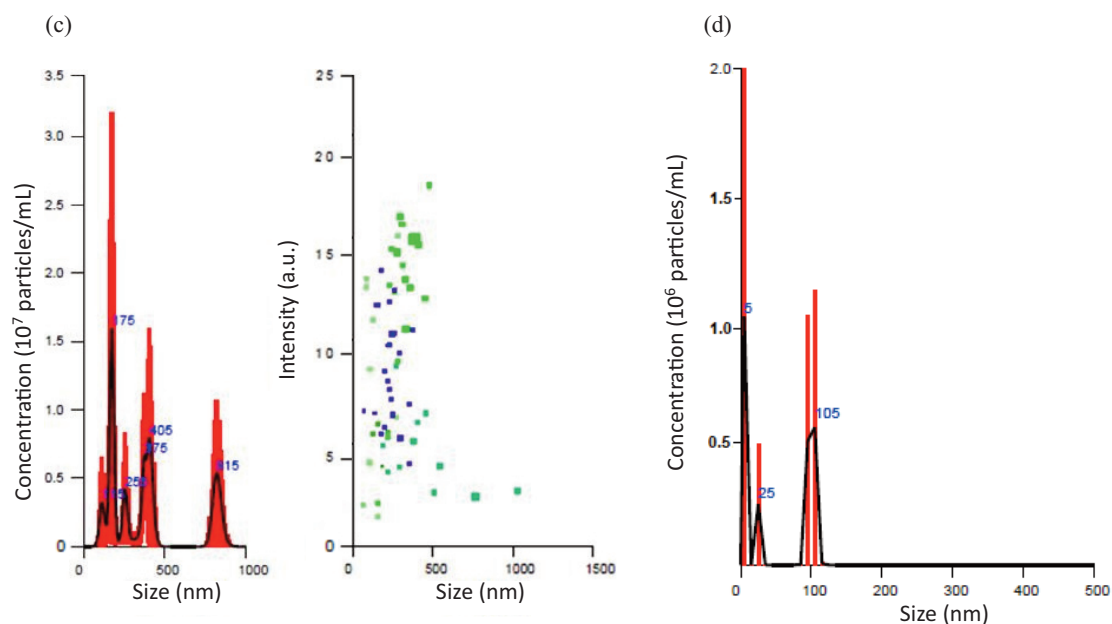
## 3. RESULTS AND DISCUSSION

According to the results obtained in the current study (Fig. 2), the first detectable particles in the analysed samples were measured by NTA containing  $0.092 \pm 0.01$  mM of SrS<sub>(s)</sub> (pH =  $9.97 \pm 0.02$ ) and  $0.097 \pm 0.01$  mM of CaS<sub>(s)</sub> (pH =  $9.94 \pm 0.02$ ) or above the aforesaid salt amount, which were in the concentration range about 18



Particle size (nm) and distribution at  $[\text{SrS}] = 0.092 \pm 0.01$  mM ( $\text{pH} = 9.97 \pm 0.02$ ); the average concentration of SrS particles is  $5.41 \pm 4.38 \cdot 10^6$  per mL.

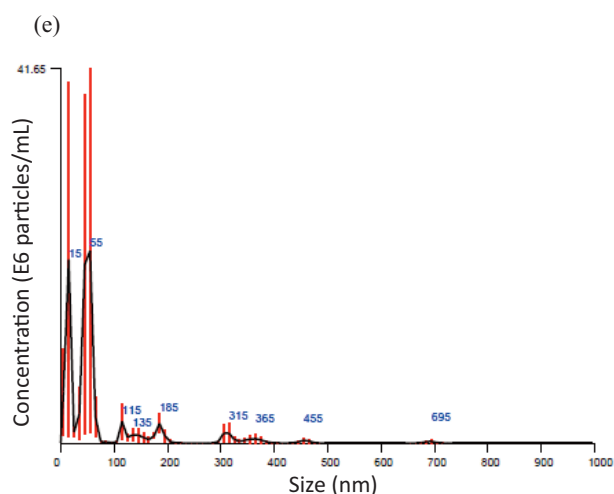
Particle size (nm) and distribution at  $[\text{SrS}] = 0.836 \pm 0.01$  mM ( $\text{pH} = 11.07 \pm 0.02$ ); the average concentration of particles is  $1.64 \pm 0.71 \cdot 10^7$  per mL.



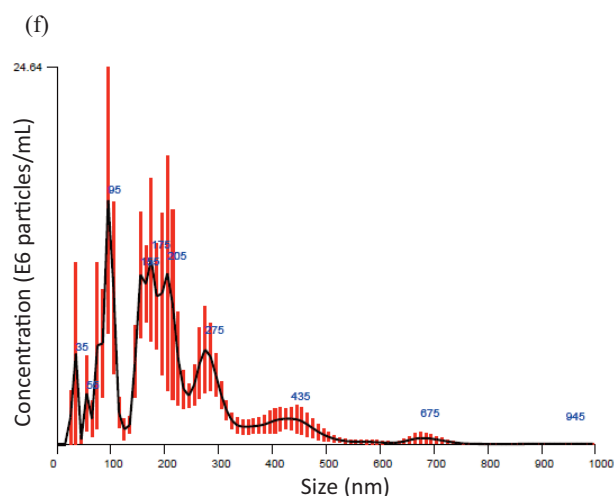
Particle size (nm) and distribution at  $[\text{SrS}] = 1.671 \pm 0.01$  mM ( $\text{pH} = 11.18 \pm 0.02$ ); the average concentration of particles is  $1.74 \pm 0.61 \cdot 10^7$  per mL.

Particle size (nm) and distribution at  $[\text{CaS}] = 0.097 \pm 0.01$  mM ( $\text{pH} = 9.94 \pm 0.02$ ), the average concentration of CaS particles is  $1.35 \pm 0.57 \cdot 10^6$  per mL.

**Fig. 2.** Size distribution and the average concentration of particles from the NTA measurements in the closed equilibrium systems of  $\text{H}_2\text{O}$ –SrS (at  $[\text{SrS}] = 0.092$ – $1.671(\pm 0.01)$ ;  $\text{pH} = 9.97$ – $11.18(\pm 0.02)$ ) and  $\text{H}_2\text{O}$ –CaS (at  $[\text{CaS}] = 0.097$ – $1.733(\pm 0.01)$ ;  $\text{pH} = 9.94$ – $11.26(\pm 0.02)$ ) at  $25 \pm 0.2$  °C. Red error bars indicate the standard error of the average concentration of particles in the measured systems. (Continued on the next page.)



Particle size (nm) and distribution at  $[\text{CaS}] = 1.388 \pm 0.01$  mM ( $\text{pH} = 11.17 \pm 0.02$ ), the average concentration of particles is  $9.07 \pm 3.96 \cdot 10^7$  per mL.



Particle size (nm) and distribution at  $[\text{CaS}] = 1.733 \pm 0.01$  mM ( $\text{pH} = 11.26 \pm 0.02$ ), the average concentration of particles is  $2.09 \pm 0.19 \cdot 10^8$  per mL.

**Fig. 2.** Continued.

times lower than our previously determined values at  $[\text{SrS}] = 1.671$  mM and  $[\text{CaS}] = 1.733$  mM ( $\text{pH} = 11.22 \pm 0.04$ ) [6,9]. Up to these amounts of added salt (SrS or CaS) in the closed equilibrium systems of  $\text{H}_2\text{O}$ –SrS and  $\text{H}_2\text{O}$ –CaS, all particles were dissolved in aqueous media due to the better solubility of smaller (nano-size) particles in the nanoscale region. No particles were detected by the NTA method below the concentrations stated above. In addition, the occurrence of nanoparticles was related to an increase in the concentration of  $\text{Sr}^{2+}$  and  $\text{Ca}^{2+}$  ions and the increase in the pH values of these equilibrium systems when an additional amount of salt (SrS or CaS) was dissolved [6,9,19]. As shown in Fig. 2 (a–f), the average concentration and size of the formed particles in these equilibrium systems increased upon adding more salt into deoxygenated MilliQ water mainly due to the coagulation of smaller particles into larger ones after additional salt was dissolved. The resultant overall decreased concentration ratio of the formed particles to the amount of the added SrS (Fig. 2: a, b, c) or CaS (Fig. 2: d, e, f) is depicted for these closed equilibrium systems.

The larger particles (size  $\geq 450$  nm) in the measured aqueous solutions of SrS and CaS were also visible due to the Tyndall effect present in colloidal systems [12,28]. Thus, the validity of particle size distributions for a sample depended on the accurate sizing of particles as well as on precise concentration measurements. As seen in Fig. 3, at lower salt concentration ( $[\text{SrS}]$  or  $[\text{CaS}] \leq 0.1$  mM) dissolved ions (or molecules) and their pairs were first formed after dissolution in aqueous media. As the smallest size of the nanoparticles detected by the NanoSight

LM10 viewing unit was 10 nm or above, they were seen in the observed equilibrium systems at about ( $[\text{SrS}]$  or  $[\text{CaS}] \geq 0.1$  mM). Disordered aggregates and crystals (after exceeding the value of the corresponding  $K_{\text{SP}}$ ) were formed at a larger amount of salt added into the closed equilibrium systems of  $\text{H}_2\text{O}$ –SrS or  $\text{H}_2\text{O}$ –CaS due to the coagulation of nanoparticles.

According to the relevant literature data, the measurement accuracy of the NTA instrument is generally within 5% of the expected particle size once correct hardware and software settings have been applied [25,29,30]. However, previous studies have indicated that the NTA instruments used for concentration measurements have still shown low precision, due to the variation in the number of particles detected between video replicate measurements of the same sample. For low particle counts it has been suggested that increasing video replicates (e.g. from 5 to 15 times) could lead to more precise concentration measurements [26,29,31]. In order to receive a sufficient confidence level ( $p < 0.05$ ) and an adequate agreement between the replicates of measurements, the prepared samples were injected five times with three repetitions for each measurement. Moreover, the mean results were then calculated and presented by the NTA instrument software. As seen in the photo captured by the NTA instrument (Fig. 4), it allowed the distinction of two or more light scattering centres for very large aggregates ( $>1$   $\mu\text{m}$ ), which suggests that they were formed by the assembly of smaller aggregates. However, the brightness of such large particles interferes with the optimization of the instrument settings, making smaller aggregates more difficult to detect.

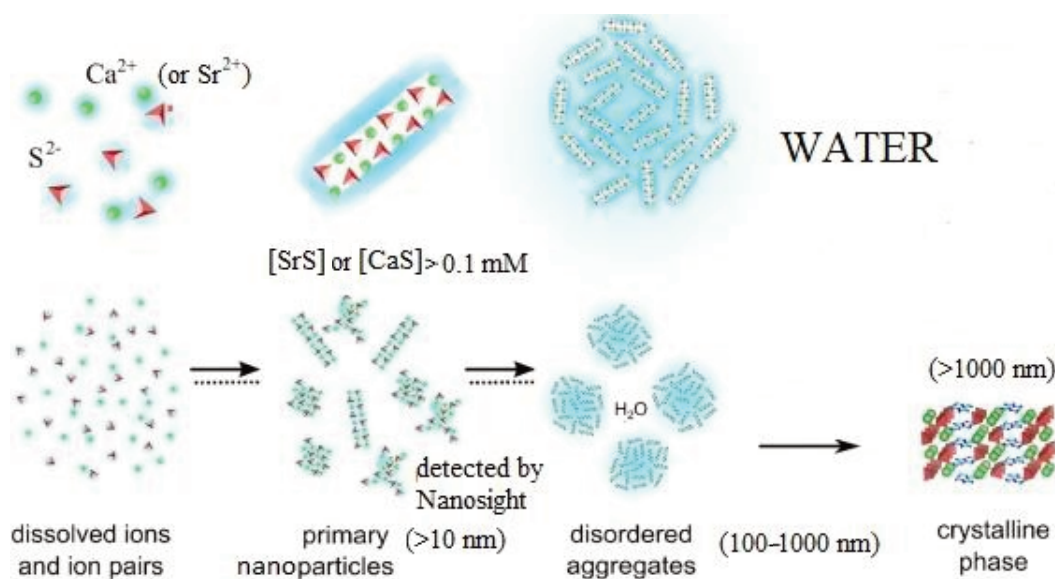


Fig. 3. Relation between the dissolved  $[\text{SrS}]_{(s)}$  or  $[\text{CaS}]_{(s)}$  and the size of the formed particles in aqueous media.



Fig. 4. Captured image of the formed SrS particles (surrounded by a series of diffraction rings) in MilliQ water in the NTA video frame.

#### 4. CONCLUSIONS

In this study, the formed particles in the closed equilibrium systems of  $\text{H}_2\text{O}$ – $\text{SrS}$  and  $\text{H}_2\text{O}$ – $\text{CaS}$  have been investigated by using the Nanosight<sup>®</sup> LM10 apparatus intended for their real-time visualization, sizing, and counting. The measured values of pHs and the quantity of the formed particles increased when an additional amount of salt was added into these closed equilibrium systems. The first particles appeared in the analysed samples containing  $0.092 \pm 0.01 \text{ mM}$  of  $\text{SrS}_{(s)}$  ( $\text{pH} = 9.97 \pm 0.02$ ) and  $0.097 \pm 0.01 \text{ mM}$  of  $\text{CaS}_{(s)}$  ( $\text{pH} = 9.94 \pm 0.02$ ) or above the aforesaid salt amount, which was about 18 times lower than our previously

determined values of solubilities of  $[\text{SrS}] = 1.671 \text{ mM}$  and  $[\text{CaS}] = 1.733 \text{ mM}$  ( $\text{pH} = 11.22 \pm 0.04$ ). For the increased amounts of added salt in the closed equilibrium systems, all particles dissolved due to the better solubility of smaller ones, which is related to their better solubility in aqueous media and the increase in the  $K_{\text{SP}}$  value. Thus, this principle allows to calculate the  $K_{\text{SP}}$  value for nanoscale particles in different equilibrium systems by using the NTA method, which is suitable for both monodisperse and polydisperse samples because it has a substantially better peak resolution compared to other similar techniques intended for their characterization in liquid suspension.

#### ACKNOWLEDGEMENTS

The study was supported by the following projects: SLTKT16012 and IUT20-16. The publication costs of this article were partially covered by the Estonian Academy of Sciences.

#### REFERENCES

- Holleman, A. F., Wiberg, E., and Wiberg, N. *Inorganic Chemistry*, 1st ed. Academic Press, San Diego, 2001.
- Douglas, B. E., McDaniel, D. H., and Alexander J. J. *Concepts and models of inorganic chemistry*, 2nd ed. John Wiley and Sons, Inc., New York, 1983.
- Lide, D. R. (ed.). *CRC Handbook of Chemistry and Physics*, 87th ed. CRC Press, Boca Raton, FL, 2006.
- LeBlanc, S. E., and Fogler, H. S. Dissolution of powdered minerals: the effect of polydispersity. *AIChE J.*, 1989, **35**(5), 865–868.

5. MacMillan, J. P., Park, J. W., Gerstenberg, R., Wagner, H., Köhler, K., and Wallbrecht, P. *Strontium and Strontium Compounds*. Wiley Online Library, 2000, [https://doi.org/10.1002/14356007.a25\\_321](https://doi.org/10.1002/14356007.a25_321)
6. Uiga, K., Tenno, T., Zekker, I., and Tenno, T. Dissolution modeling and potentiometric measurements of the SrS–H<sub>2</sub>O–gas system at normal pressure and temperature at salt concentrations of 0.125–2.924 mM. *J. Sulfur Chem.*, 2011, **32**(2), 137–149.
7. Patnaik, P. *Handbook of Inorganic chemicals*. The McGraw-Hill Companies, Inc., USA, 2003.
8. Zvimba, J. N., Mulopo, J., De Beer, M., Bologo, L., and Mashego, M. The dissolution characteristics of calcium sulfide and utilization as a precipitation agent in acidic wastewater effluent treatment. *Water Sci. Technol.*, 2011, **63**(12), 2860–2866, <https://doi.org/10.2166/wst.2011.599>
9. Zekker, I., Tenno, T., Selberg, A., and Uiga, K. Dissolution modeling and experimental measurement of CaS–H<sub>2</sub>O binary system. *Chin. J. Chem.*, 2011, **29**(11), 2327–2336.
10. Mölder, L., Elenurm, A., and Tamvelius, H. Sulphur compounds in a hydraulic ash-disposal system. *Proc. Estonian Acad. Sci. Chem.*, 1995, **44**(2–3), 207–211.
11. Yongsiri, C., Hvitved-Jacobsen, T., Vollertsen, J., and Tanaka, N. Introducing the emission process of hydrogen sulfide to a sewer process model (WATS). *Water Sci. Technol.*, 2003, **47**(4), 85–92.
12. Hiemenz, P. C. and Rajagopalan, R. *Principles of Colloid and Surface Chemistry*, 3rd ed. CRC Press, Boca Raton, FL, 1997.
13. Chizhik, V. I., Egorov, A. V., Pavlova, M. S., Egorova, M. I., and Donets, A. V. Structure of hydration shell of calcium cation by NMR relaxation, Car-Parrinello molecular dynamics and quantum-chemical calculations. *J. Mol. Liq.*, 2016, **224**(Part A), 730–736.
14. Luz, E. P. C. G., Borges, M. F., Andrade, F. K., Rosa, M. F., Infantes-Molina, A., Rodríguez-Castellón, E., and Vieira, R. S. Strontium delivery systems based on bacterial cellulose and hydroxyapatite for guided bone regeneration. *Cellulose*, 2018, **25**, 6661–6679, <https://doi.org/10.1007/s10570-018-2008-8>
15. Sennett, P. and Olivier, J. P. Colloidal dispersions, electrokinetic effects, and the concept of zeta potential. *Ind. Eng. Chem.* 1965, **57**(8), 32–50, <https://doi.org/10.1021/ie50668a007>
16. Zumdahl, S. S. *Chemical Principles*. 2nd ed. D. C. Heath and Co., Lexington, MA, 1995.
17. Mullin, J. W. *Crystallization*, 4th ed. Butterworth-Heinemann, Oxford, 2001.
18. Tenno, T., Uiga, K., Mashirin, A., Zekker, I., and Rikmann, E. Modeling closed equilibrium systems of H<sub>2</sub>O–dissolved CO<sub>2</sub>–solid CaCO<sub>3</sub>. *J. Phys. Chem. A.*, 2017, **121**(16), 3094–3100.
19. Tenno T., Rikmann, E., Zekker, I., and Tenno T. Modelling the solubility of sparingly soluble compounds depending on their particles size. *Proc. Estonian Acad. Sci.*, 2018, **67**(3), 300–302, <https://doi.org/10.3176/proc.2018.3.10>
20. Yan, H., Wang, X.-S. and Zhu, R.-Z. Derivation of the Kelvin Equation. *Acta Phys. Chim. Sin.*, 2009, **25**(4), 640–644.
21. Wu, W. and Nancollas, G. H. A new understanding of the relationship between solubility and particle size. *J. Solution Chem.*, 1998, **27**(6), 521–531.
22. Wright, M. Nanoparticle Tracking Analysis for the Multiparameter Characterization and Counting of Nanoparticle Suspensions. In *Nanoparticles in Biology and Medicine. Methods in Molecular Biology* (Soloviev, M., ed.), vol. 906, Human Press, Totowa, NJ, 2012, 511–524, [https://doi.org/10.1007/978-1-61779-953-2\\_41](https://doi.org/10.1007/978-1-61779-953-2_41)
23. Maguire, C. M., Rösslein, M., Wick, P., and Prina-Mello, A. Characterisation of particles in solution – a perspective on light scattering and comparative technologies. *Sci. Technol. Adv. Mater.*, 2018, **19**(1), 732–745, <https://doi.org/10.1080/14686996.2018.1517587>
24. Hole, P., Sillence, K., Hannell, C., Maguire, C. M., Roesslein, M., Suarez, G. et al. Interlaboratory comparison of size measurements on nanoparticles using nanoparticle tracking analysis (NTA). *J. Nanopart. Res.*, 2013, **15**(12), 2101–2112.
25. Gardiner, C., Ferreira, Y. J., Dragovic, R. A., Redman, C. W. G., and Sargent, I. L. Extracellular vesicle sizing and enumeration by nanoparticle tracking analysis. *J. Extracell. Vesicles*, 2013, **2**(1), <https://doi.org/10.3402/jev.v2i0.19671>
26. Filipe, V., Hawe, A., and Jiskoot, W. Critical evaluation of nanoparticle tracking analysis (NTA) by NanoSight for the measurement of nanoparticles and protein aggregates. *Pharm. Res.*, 2010, **27**(5), 796–810, <https://doi.org/10.1007/s11095-010-0073-2>
27. Steinhauser, M. O. and Hiermaier, S. A review of computational methods in materials science: examples from shock-wave and polymer physics. *Int. J. Mol. Sci.*, 2009, **10**(12), 5135–5216, <https://doi.org/10.3390/ijms10125135>
28. Young, R. O. Colloids and colloidal systems in human health and nutrition. *Int. J. Complement. Altern. Med.*, 2016, **3**(6), <https://doi.org/10.15406/ijcam.2016.03.00095>
29. Du, S., Kendall, K., Morris, S., and Sweet, C. Measuring number-concentrations of nanoparticles and viruses in liquids on-line. *J. Chem. Technol. Biotechnol.*, 2010, **85**(9), 1223–1228, <https://doi.org/10.1002/jctb.2421>
30. Röding, M., Zagato, E., Remaut, K., and Braeckmans, K. Approximate Bayesian computation for estimating number concentrations of monodisperse nanoparticles in suspension by optical microscopy. *Phys. Rev. E*, 2016, **93**(6), <https://doi.org/10.1103/PhysRevE.93.063311>
31. Parsons, M. E. M., McParland, D., Szklanna, P. B., Guang, M. H. Z., O’Connell, K., O’Connor, H. D. et al. A protocol for improved precision and increased confidence in nanoparticle tracking analysis concentration measurements between 50 and 120 nm in biological fluids. *Front Cardiovasc. Med.*, 2017, **4**(68), <https://doi.org/10.3389/fcvm.2017.00068>

## Vähelahustuvate SrS ja CaS osakeste määramine ning lahustuvus vees sõltuvalt nende jaotumisest suuruse järgi

Kalev Uiga, Ergo Rikmann, Ivar Zekker ja Toomas Tenno

Käesoleva uurimistöö eesmärk oli uurida sarnaste keemiliste omadustega (näiteks struktuur, ioonraadius) SrS ja CaS (vähelahustuvad leelismuldmetallide sulfiidid) lahustumist ja moodustunud osakeste jaotumist MilliQ ülipuhtas vees sõltuvalt lisatud soola kogusest ning suurusest. Antud suletud tasakaalulistes süsteemides H<sub>2</sub>O–SrS ja H<sub>2</sub>O–CaS mõõdetud pH väärtused suurenesid täiendava koguse soola lisamisel, kuna moodustunud osakeste arv kasvas. Esimesed nanoosakesed (detekteeritud Nanosight<sup>®</sup> LM10 abil) ilmusid ettevalmistatud vesilahuse proovides, mis sisaldasid 0,092 ± 0,01 mM SrS<sub>(s)</sub> (pH = 9,97 ± 0,02) ja 0,097 ± 0,01 mM CaS<sub>(s)</sub> (pH = 9,94 ± 0,02) või enam antud soolade kogustest, mis on umbes 18 korda väiksem kui varasemates uuringutes saadud vastavad lahustuvuse väärtused ([SrS] = 1,671 mM; [CaS] = 1,733 mM (pH = 11,22 ± 0,04)). Nendest lisatud soola kogustest väiksemate väärtuste korral olid kõik uuritud süsteemides moodustunud peenosakesed lahustunud nende suurema eripinna ja sellest tingitud parema lahustuvuse tõttu, mis on seotud ka nende tasakaaluliste süsteemide lahustuvuskorrutiste ( $K_{SP}$ ) väärtuse tõusuga. Antud seaduspära võimaldaks arvutada viimase väärtust ka nanomõõtmets osakeste korral eri tasakaalulistes süsteemides NTA meetodi abil, mis sobib nende suuruse ja jaotumise analüüsimiseks.